

(NASA-CR-197503) ACTIVE CHLORINE  
AND NITRIC OXIDE FORMATION FROM  
CHEMICAL ROCKET PLUME AFTERBURNING  
(Pennsylvania State Univ.) 14 p

N96-16580

Unclass

63/20 0065139

D. M. Leone\* and S. R. Turns†  
 Propulsion Engineering Research Center  
 Department of Mechanical Engineering  
 The Pennsylvania State University  
 University Park, PA 16802

NAGW-1356  
 IN-20-CR  
 © OVERRIDE  
 65139  
 P. 14

### Abstract

Chlorine and oxides of nitrogen ( $\text{NO}_x$ ) released into the atmosphere contribute to acid rain (ground level or low-altitude sources) and ozone depletion from the stratosphere (high-altitude sources). Rocket engines have the potential for forming or activating these pollutants in the rocket plume. For instance,  $\text{H}_2/\text{O}_2$  rockets can produce thermal  $\text{NO}_x$  in their plumes. Emphasis, in the past, has been placed on determining the impact of chlorine release on the stratosphere. To date, very little, if any, information is available to understand what contribution  $\text{NO}_x$  emissions from ground-based engine testing and actual rocket launches have on the atmosphere.

The goal of this work is to estimate the afterburning emissions from chemical rocket plumes and determine their local stratospheric impact. Our study focuses on the Space Shuttle rocket motors, which include both the solid-rocket-boosters (SRBs) and the liquid propellant main engines (SSMEs). Rocket plume afterburning is modeled employing a one-dimensional model incorporating two chemical kinetic systems: chemical and thermal equilibrium with overlaid nitric oxide chemical kinetics (semi-equilibrium) and full finite-rate chemical kinetics. Additionally, the local atmospheric impact immediately following a launch is modeled as the emissions diffuse and chemically react in the stratosphere.

### Nomenclature

variable	definition	units
b	plume half-width	m
$C_1$	spatial transform variable	-
dx	width of plume control volume	m
$E_1$	entrainment constant	-
$EI_i$	species i emission index	g i/kg fuel
h $\nu$	photon	-
$h_i$	species i enthalpy	J/kg
K	eddy diffusion model constant	m/s
$K_{\pi}$	eddy diffusion coefficient	$\text{m}^2/\text{s}$

- \* Research Engineer, Southwest Research Institute, San Antonio, TX 78228, AIAA Member  
 † Professor, AIAA Member

variable	definition	units
$\dot{m}$	mass flowrate	kg/s
$n_i$	species i mean molar conc.	$\text{kmol}/\text{m}^3$
p	atmospheric pressure	kPa
r	radial coordinate	m
$r_o$	plume afterburning initial radius	m
$R_o$	plume diffusion initial radius	m
t	time	s
T	plume temperature	K
u	plume mean velocity	m/s
$\dot{\omega}$	molar production rate	$\text{kmol}/\text{m}^3\text{-s}$
x	axial coordinate	m
X	catalyst	-
$y_i$	species or elemental mass fraction	-

subscript	definition
r	radial coordinate
x	axial location x
$\infty$	freestream

superscript	definition
'	fluctuation

### Background

Accounting for the effects of chemical rockets on the environment is not new. During the design and analysis of the Space Shuttle, many environmental issues were addressed. The results of these studies are published in the Space Shuttle Program Final Environmental Impact Statement<sup>1</sup> and by Potter<sup>2,3</sup>.

A major emphasis of the Space Shuttle Program Final Environmental Impact Statement and Potter's work centers on the environmental impact due to exhaust from the Space Shuttle Solid Rocket Boosters (SRBs). The Space Shuttle's Main Engines (SSMEs) burn liquid hydrogen and oxygen and are generally considered pollution free, although the afterburning could produce some thermal oxides of nitrogen.<sup>4</sup>

### Propellants

The three rocket propellant types are solid, liquid and hybrid. A solid rocket propellant is generally a solidified matrix of fuel and oxidizer loaded with metal particles. The most common solid propellant matrix is perchlorate oxidizer and a polymer fuel heavily loaded

with powdered aluminum.<sup>4</sup> This type of solid rocket fuel is utilized in both the Space Shuttle SRBs and the Titan-IV SRMs, the two largest launch systems. The principle nozzle exit plane products of combustion are hydrogen chloride, solid aluminum oxide particules, water, hydrogen, carbon monoxide, and carbon dioxide.<sup>4</sup> A more complete set of combustion products is listed in Table 1.

Table 1. Equilibrium products at the nozzle exit.<sup>4,5</sup>

Propellant	Major Products	Minor Products
Typical solid	HCl, Al <sub>2</sub> O <sub>3</sub> , H <sub>2</sub> , H <sub>2</sub> O, CO, CO <sub>2</sub>	Cl, Cl <sub>2</sub> , FeCl <sub>2</sub> , H, OH, N <sub>2</sub> , NO
LO <sub>x</sub> /LH <sub>2</sub>	H <sub>2</sub> , H <sub>2</sub> O	H, OH, HO <sub>2</sub>

The current generation of major liquid propellants are nitrogen tetroxide (N<sub>2</sub>O<sub>4</sub>) and aerzine fuel, liquid oxygen (LO<sub>x</sub>) and kerosene (RP-1), and LO<sub>x</sub> and liquid hydrogen (LH<sub>2</sub>).<sup>4</sup> Fuel type is selected based upon the rocket application. The liquid propellants' major combustion products are listed in Tables 1 and 2.

Table 2. Liquid propellant primary products of combustion.<sup>4</sup>

Liquid Propellant	Major Products
LO <sub>x</sub> /kerosene	H <sub>2</sub> , H <sub>2</sub> O, CO, CO <sub>2</sub>
Nitrogen tetroxide/aerzine	H <sub>2</sub> , H <sub>2</sub> O, CO, CO <sub>2</sub> , N <sub>2</sub>

The hybrid propellant is a combination of solid and liquid fuel and oxidizer. Generally the hybrid propellant is a solid fuel matrix, usually polybutadiene, and a liquid oxidizer such as LO<sub>x</sub>. The typical combustion products are similar to those of the LO<sub>x</sub>/kerosene propellant listed in Table 2. Hybrid propellants are still under development.

### Afterburning

The products of combustion listed in Tables 1 and 2 are the chemical species at the nozzle exit plane. The gases exit the nozzle at high velocities, and for the Shuttle SRBs, high temperatures as well. Typical SRB exit plane velocities and temperatures are 2400 m/s and 2300 K respectively.<sup>5</sup> The exhaust gases travel into the open atmosphere in a plume, engulfing and mixing

surrounding air. The fuel-rich plume continues to react (afterburning), with the addition of atmospheric oxygen further completing combustion, i.e., converting carbon monoxide to carbon dioxide and hydrogen to water vapor. Afterburning holds the plume temperature elevated for extended periods of time, allowing other chemical reactions to occur.

Gomberg and Stewart studied plume afterburning in solid rocket motors.<sup>5</sup> They modeled the formation of oxides of nitrogen and chlorine repartitioning from plume afterburning for the Space Shuttle SRBs and Titan III-C SRMs. Their analysis utilized the Low Altitude Plume Program (LAPP). LAPP is a two-dimensional, axisymmetric, turbulent, compressible code incorporating finite-rate chemical kinetics. The chemical mechanism describing the plume afterburning employed 36 reactions including 18 species.

Gomberg and Stewart found that production of oxides of nitrogen decreases with altitude. At sea level, the Space Shuttle SRB nitric oxide emission index is nearly 10 g NO/kg exhaust, while at 15 km the nitric oxide emission index is approximately 1 g NO/kg exhaust. At high altitudes, the plume temperature decreases due to the initial expansion to match local atmospheric pressure. This lower plume temperature prevents afterburning nitric oxide formation. In contrast to the nitric oxide trend, Gomberg and Stewart's results show hydrogen chloride (HCl) conversion to active chlorine (Cl<sub>2</sub> and Cl) increases with altitude.

Since 1976, when Gomberg and Stewart's study was performed, advances have been made in understanding the chemical kinetics of afterburning; therefore, their conclusions may be modified.

A shortcoming in Gomberg and Stewart's work is LAPP's lack of sophistication to account accurately for large pressure differences between the nozzle exit and the local atmosphere. These large pressure differences exist for the SRM's operating at high altitudes. Gomberg and Stewart assume the exhaust undergoes an isentropic expansion to match the local atmospheric pressure. The expansion decreases the plume temperature and increases velocity. Gomberg and Stewart also assume that plume chemical composition does not change through the isentropic expansion. Therefore, the expanded plume composition is not initially in chemical equilibrium.

Dash et al. performed a study to assess the accuracy of assuming the exhaust undergoes a purely isentropic expansion.<sup>6</sup> They looked at the differences

between isentropic and nonisentropic equilibrated plume temperatures, velocities, and radii. Solid propellant motor exit-plane pressures are generally near one atmosphere; therefore, at altitudes above sea level, the nozzle exit-plane gases are underexpanded.

For altitudes of 15 km, Dash et al. found the isentropic expansion predicts a plume temperature within 5% of the nonisentropic expansion prediction; while at an altitude of 50 km, the isentropic expansion predicts a plume temperature nearly 20% lower than the nonisentropic expansion prediction. Since Gomberg and Stewart recognized the limitations of their calculations, they ran afterburning test cases only up to altitudes of 15 km for the Space Shuttle SRB and 18 km for the Titan-IIIc SRM.<sup>5</sup>

The standardized plume flowfield (SPF) code goes beyond LAPP by including the effects of shock waves and multidimensionality on plume afterburning. The third generation of SPF was employed by Denison et al. to predict final exhaust products from a hypothetical TRW solid propellant motor.<sup>8</sup> Their chemical kinetic model to predict the plume afterburning incorporates 46 reactions including 23 species. The hypothetical TRW solid rocket motor is about four times smaller than a Space Shuttle SRB. Denison et al. analyzed plume afterburning at altitudes up to 30 km, where the plume's nonisentropic expansion can have a substantial impact on the plume properties. Their results show, like Gomberg and Stewart's, that chlorine activation ( $\text{HCl}$  to  $\text{Cl}$  or  $\text{Cl}_2$ ) increases with altitude, and at both altitudes studied (18 km & 30 km), negligible oxides of nitrogen are created in the plume.<sup>5</sup>

In contrast to SRMs, little information on  $\text{NO}_x$  formation from plume afterburning for liquid or hybrid propellants is available in the literature. Qualitatively, afterburning will further complete combustion and produce oxides of nitrogen and oxides of hydrogen. Chlorine and aluminum are absent in the propellants of current-generation liquid and developmental hybrid propellants.<sup>4</sup>

### Atmospheric Effects

Many literature sources contain information on impact of chemical rockets on the surface layer and troposphere. For instance, the Space Shuttle Program Final Environmental Impact Statement contains information on possible effects from the Space Shuttle.<sup>1</sup> The ground cloud and the exhaust trail left in the troposphere contains products that can impact the environment. The initial advection and dispersion of

the ground cloud deposits exhaust directly on the earth's surface.

In the troposphere and boundary layer, oxides of nitrogen and chlorine are known precursors to ozone production.<sup>9</sup> Little information in the literature exists predicting tropospheric ozone created through the chlorine route. The chlorofluorocarbons (CFCs) are stable and insoluble molecules in the troposphere, but the chlorine from solid propellant rocket exhaust is soluble and active in the troposphere.

It is well understood that the nitrogen oxide mechanism for producing ozone is dependent upon the ratio of  $\text{NO}_2$  to  $\text{NO}$  ( $\text{NO}_x$  ratio). Other species in the exhaust trail and ground cloud can increase the  $\text{NO}_x$  ratio. For instance, carbon monoxide oxidizes in the atmosphere through the net reaction

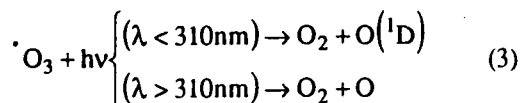


where the hydroperoxyl radical then reacts with  $\text{NO}$  forming  $\text{NO}_2$ .<sup>9</sup> This increases the  $\text{NO}_x$  ratio with no loss in hydroxyl radicals.

The stratosphere is characterized by a positive temperature gradient with increasing altitude. Due to the thermal stratification, vertical mixing is relatively slow. Although the vertical temperature increase is only approximately 25%, the atmospheric pressure decreases by nearly 10,000%.

Chemical rockets pass through the stratosphere depositing exhaust directly. The exhaust mixes on a local and, subsequently, on a global scale. The exhaust can potentially alter natural stratospheric chemistry.

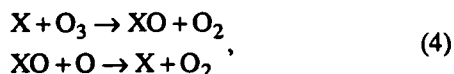
The temperature of the stratosphere increases with altitude because of heating from photo-absorption of ultraviolet light by ozone. Ozone is created and destroyed primarily through the chemical reactions:<sup>10</sup>



The excited oxygen atom created by reaction 3 can react with water, hydrogen, or methane creating hydroxyl radicals.

Another major route for destruction of ozone lies in catalytic reactions. Ozone is predominately destroyed through catalytic reactions from three

families: active chlorine, odd hydrogen and odd nitrogen. The term "family" refers to a group of species that react readily among family members, while generally reacting slowly with species outside the family. The species associated with each of the three families are listed in Table 3. The catalyst reactions are usually regarded as the fastest and most destructive reactions to ozone. The known catalyst cycle is



where X can be Cl, N, or H. All reactions result in a net destruction of ozone with no loss in the catalyst. The reaction cycle ceases once the catalyst undergoes a reaction forming a non-catalyst species.

Table 3. Predominant species of the active chlorine and odd nitrogen and hydrogen families. Italicized species are considered reservoir species.

Family	Species
Active Chlorine ( $Cl_x$ )	Cl, ClO, HOCl, ClO <sub>2</sub> , <i>HCl, ClONO<sub>2</sub></i>
Odd Nitrogen (NO <sub>x</sub> )	NO, NO <sub>2</sub> , N, NO <sub>3</sub> , <i>N<sub>2</sub>O<sub>5</sub>, HO<sub>2</sub>NO<sub>2</sub>, HNO<sub>3</sub>, ClONO<sub>2</sub></i>
Odd Hydrogen (HO <sub>x</sub> )	OH, HO <sub>2</sub> , H <sub>2</sub> O <sub>2</sub> , H, <i>HOCl, HO<sub>2</sub>NO<sub>2</sub>, HNO<sub>3</sub></i>

### Local Plume Dispersion

In recent work, Denison et al. modeled the local plume diffusion of a TRW hypothetical solid rocket motor.<sup>8</sup> The chemical kinetics model incorporates 17 reactions including 19 species. The chlorine catalyst reaction dominates ozone destruction because of the large atomic chlorine concentrations in the plume of the solid rocket motor.

Local atomic chlorine is produced from two primary sources: hydrogen chloride during the afterburning, and photo-dissociation of diatomic chlorine during the local diffusion. In the stratosphere, the diatomic chlorine photo-dissociation reaction has a time constant of approximately 300 sec.<sup>10</sup> Due to the extended time required to activate hydrogen chloride in the diffusing plume, hydrogen chloride is ineffective at destroying local ozone.

Denison et al.'s model shows that the rocket exhaust can greatly affect local ozone.<sup>8</sup> Immediately

following plume exhaust injection, ozone is significantly reduced out to radii of 100 m for up to five minutes, but radii greater than 900 m show little ozone depletion at any time. In studying the effects of chemical rockets on local ozone, plume afterburning is very important. When afterburning is neglected in Denison et al.'s diffusion model, no significant active chlorine (Cl or Cl<sub>2</sub>) is present in the exhaust plume, and ozone depletion is minimal.

Since the hypothetical TRW solid rocket motor analyzed is approximately four times smaller than one Shuttle SRB, the effect the larger engines may have on local ozone remains to be seen.

Experimental evidence agrees qualitatively with the local diffusion model predictions. The exhaust trail of a Titan-III solid rocket was sampled by an aircraft at an altitude of 18 km, 13 minutes after launch; the results showed a local reduction of ozone greater than 40%.<sup>11</sup>

Local ozone depletion will not create an ozone hole over the launch site as rockets pass through the stratosphere on a slant path. This evidence agrees with Total Ozone Mapping Spectrometer (TOMS) measurements showing no significant ozone depletion following the launch of the Space Shuttle.<sup>12</sup>

### Global Plume Dispersion

Over time, the localized exhaust species will be transported and mixed on a global scale. Much of the original analysis of the Space Shuttle's impact on the stratosphere focused on global perturbation of ozone due to chlorine deposition.

As described by reactions 4, atomic chlorine is very effective in destroying ozone; however, hydrogen chloride is relatively inactive. Hydrogen chloride can be activated by hydrogen chloride, oxygen radicals, or photons. According to Brasseur and Solomon, active chlorine is inactivated primarily through reaction with methane, but in the upper stratosphere, the hydroperoxyl radical can play a role in the deactivation.<sup>13</sup>

Chlorine is eventually removed from the stratosphere by transport to the troposphere as hydrogen chloride; hydrogen chloride is soluble and removed by wet deposition (precipitation). Unlike CFCs, the reactivity and solubility of the chlorine emitted by solid propellants prevent substantial transport from the troposphere to the stratosphere.

Recent work by Prather et al. studies the impact of chemical rocket chlorine on the stratosphere utilizing state-of-the-art models incorporating current chemical kinetics data.<sup>14</sup> This study looks at the stratospheric impact rocket launches representative of current launch rates. For this launch rate scenario, 660 Mg of chlorine are released per year. In comparison, the chemical industry releases over 1,100,000 megagrams of CFCs per year. The ambient chlorine concentration is estimated to increase by 0.5% due to the 13 launches a year, and ozone perturbations are predicted to be minimal.

With advances in understanding the seasonal ozone hole over Antarctica, scientists have discovered the importance of heterogeneous chemistry. Ice clouds formed in the cold stratosphere provide nucleation sites for enhanced conversion of inactive hydrogen chloride into active chlorine.<sup>8</sup> These reactions remove nitric oxide from the stratosphere; thereby eliminating the reaction



which inactivates the active chlorine and nitrogen molecules. The active chlorine molecule then destroys ozone unchallenged.

Aluminum oxide released from solid rocket motors may provide both nucleation sites for increased ice formation and, analogous to ice, provide nucleation sites for stratospheric heterogeneous chemistry. Recent measurements show stratospheric aluminum oxide concentrations are increasing due to solid rocket motor launches and space debris.<sup>14</sup>

Calculations by Denison et al. show negligible change in local ozone depletion when aluminum oxide heterogeneous chemistry is incorporated.<sup>8</sup> According to Prather et al., global impact of aluminum oxide remains uncertain, and further experimental work is necessary to determine accurately heterogeneous reaction rates.<sup>14</sup> Small aluminum oxide particulates are filtered out of the stratosphere after dispersing hemispherically over time.<sup>15</sup> The large-diameter aluminum oxide particles (approximately greater than 1  $\mu\text{m}$  in diameter) are removed by particle sedimentation into the troposphere.<sup>14</sup>

### One-Dimensional Plume Analysis

The goal of this work is to estimate the afterburning emissions from chemical rocket plumes and determine their local stratospheric impact. A one-dimensional plume afterburning model was selected

based upon three major factors: simplicity of the conservation equations, recent turbulent jet analysis, and the ability to gain physical insight.

The assumed one-dimensionality produces simple conservation equations that allows the plume to be coupled with varying degrees of chemical kinetic complexity, while keeping the computations inexpensive. Analyses of turbulent jets by Broadwell showed that turbulent jet coherent structures reduce the radial variations of instantaneous quantities such as temperature and species concentrations; thus Broadwell's analysis provides some physical validity to the one-dimensional model.<sup>16</sup> The last factor, gaining physical insight, may seem to hold the least importance, but the knowledge gained from the one-dimensional model's physics and chemistry provides simple insight, which may be lost in more complex models. Results from a simple one-dimensional plume model can suggest direction for more sophisticated analyses.

The exhaust gases exit the nozzle, and if the exhaust pressure is slightly above atmospheric pressure, the plume undergoes an isentropic expansion. The isentropic expansion increases the jet velocity and decreases the temperature. If the exit pressure is below or greatly above atmospheric, the plume undergoes a complex series of nonisentropic shock/expansion waves. If the plume contains shockwaves, difficulties arise in predicting the initial conditions for an analysis of afterburning.

A schematic of the plume is shown in Figure 1. Assuming there are no shockwaves in the plume following initial pressure adjustments, the static pressure at any point is atmospheric. Once the exhaust pressure equilibrates, the plume undergoes a complex development period. As the exhaust gases move further downstream, they entrain air through turbulent motion and, ultimately, the plume and entrained gases are mixed down to the molecular level.

Plume temperature plays an important role in the plume conversion of exhaust constituents. Three primary elements affect the plume temperature: afterburning, dilution, and conversion of kinetic to sensible energy. During afterburning the oxygen added through entrainment reacts with any unburned fuel, thereby increasing the temperature. Air beyond the amount necessary to complete combustion dilutes the plume and decreases the temperature, which slows afterburning. Entrainment also increases the plume's mass flowrate, decreasing the velocity and converting

kinetic to sensible energy, raising the plume temperature.

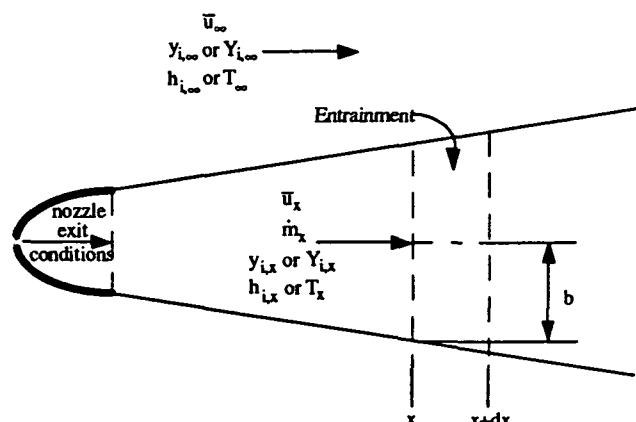


Figure 1. Schematic of plume showing integral control volume and major variables.

Following the approaches of Lutz and Broadwell, our one-dimensional model treats the plume as a perfectly-stirred reactor.<sup>17,16</sup> Two versions of the model were developed that differ in their treatment of chemistry. The first version assumes all species are in chemical equilibrium, except nitric oxide and atomic nitrogen atoms; while the second version allows for full finite-rate chemical kinetics. The conservation equations include mass, momentum, elemental mass or species mass fractions, and energy. A relationship for mass entrainment rate is needed to close the set of conservation equations. For preliminary analyses, the models employ Ricou and Spalding's findings that the mass entrainment rate far from the nozzle is constant, only depending upon nozzle exit-plane properties.<sup>18</sup> The entrainment-rate constant utilized in the one-dimensional model is set equal to that obtained by Becker and Yamazaki for turbulent propane flames.<sup>19</sup>

Thermal nitric oxide is produced by the well-known extended Zeldovich mechanism. To estimate the formation of NO, the concentrations of N, O, OH, and H are required.

The semi-equilibrium analysis uses the plume mean temperature and assumes that the species O, OH, and H are in equilibrium and N is in steady-state. To predict plume thermal NO, the semi-equilibrium version adds to the basic conservation equations an additional equation modeling NO production through the Zeldovich mechanism.

The full-kinetic version includes the Zeldovich mechanism in the chemical kinetic mechanism. For

the full description of hydrogen and carbon monoxide burning in air, neglecting formaldehyde, the chemical kinetic mechanism described by Miller and Bowman is composed of 70 elementary, single-step reactions involving 21 species.<sup>20</sup> The current chlorine chemical kinetic mechanism adds approximately 20 reactions involving 6 species.<sup>21</sup> Aluminum oxide is considered inert in both plume afterburning models.

Both one-dimensional model versions make use of published routines for the chemistry, thermodynamic properties and numerical solution techniques. The semi-equilibrium version employs STANJAN, an element potential method for chemical equilibrium calculations.<sup>22</sup> The full-kinetic version utilizes CHEMKIN-II, a FORTRAN chemical kinetics package for the analysis of gas-phase chemical kinetics.<sup>23</sup> The governing set of first-order differential equations are integrated using a stiff solver employing Gear's method.<sup>24,25</sup>

## Plume Afterburning Results and Discussion

### Shuttle SRBs

The two chemical versions of the one-dimensional model are compared with the work of Gomberg and Stewart.<sup>5</sup> To accurately compare the one-dimensional model to LAPP, the one-dimensional model uses Gomberg and Stewart's published Shuttle SRB plume initial conditions. An isentropic expansion was utilized to obtain starting line properties for altitudes above 6 km. Two additional test cases are run for higher altitudes, 20 and 30 km. Dash et al.'s results for nonisentropic plume expansions provided correction factors to use on isentropic estimates at high altitudes.<sup>6</sup>

To see the effects on the choice of reaction mechanisms, two cases of the one-dimensional full-kinetics version are run. In the first case, only Gomberg and Stewart's chemical mechanism is used. In the second case, the more recent chemical mechanisms of Miller and Bowman and DeMore et al. are applied.<sup>20,21</sup> Figures 2 and 3 show the results for both chemical mechanisms utilized by the full-kinetic version together with Gomberg and Stewart's results.

All three test findings show a dramatic increase in chlorine activation with altitude (Figure 3). The mean plume temperature decreases with altitude due to the initial plume expansion to meet atmospheric pressure; therefore, thermal nitric oxide production significantly decreases with altitude (Figure 2). The one-dimensional plume afterburning model predicts chlorine activation increases about 10-fold, while the

nitric oxide production decreases nearly 1000-fold, in going from an altitude of 0.7 to 30 km. Not shown in Figures 2 and 3 are the semi-equilibrium version results. The semi-equilibrium version predicts, unlike finite-rate chemical kinetic programs, that chlorine activation decreases with increasing altitude.

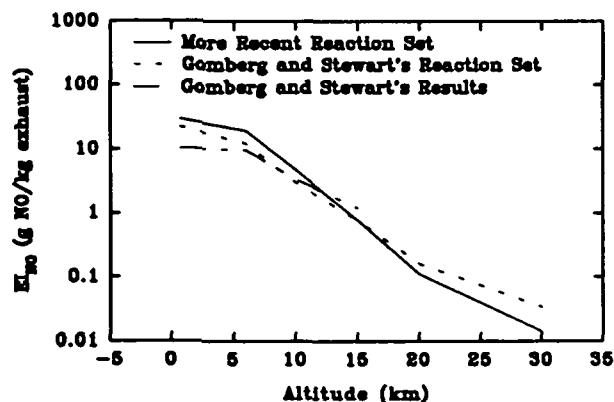


Figure 2. Nitric oxide production estimates for Shuttle SRB plume afterburning.

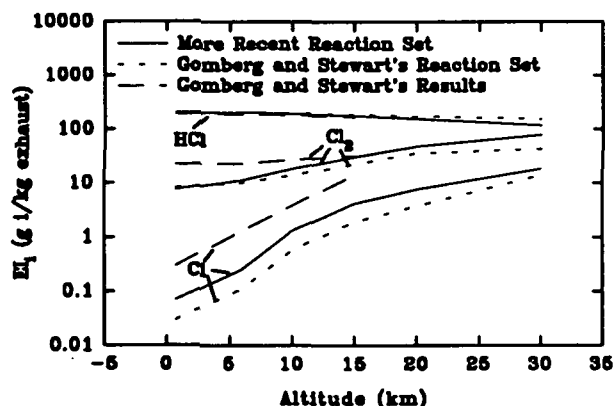


Figure 3. Chlorine activation predictions for Shuttle SRB plume afterburning. The more recent chemical mechanism results incorporate corrected starting-line plume properties.

At low altitudes, Gomberg and Stewart predicted more chlorine activation than either chemical-kinetic mechanism utilized in the one-dimensional model.<sup>5</sup> Yet, at all altitudes, the full-kinetic version utilizing Gomberg and Stewart's chemical kinetic mechanism estimates less chlorine activation than the full-kinetic version employing the more recent chemical-kinetic mechanism.

Denison et al., using the Standardized Plume Flowfield (SPF) code estimated higher amounts, of

plume chlorine activation in a hypothetical TRW SRM than predicted by our one-dimensional plume model.<sup>8</sup> For the TRW SRM operating at 30 km, Denison et al. predicted that the final chlorinated species is predominately activated ( $\text{Cl}$  or  $\text{Cl}_2$ ). Utilizing the corrected Shuttle SRB plume starting-line properties, our one-dimensional model predicts that the chlorine remains predominately inactive ( $\text{HCl}$ ).

### SSMEs

The one-dimensional model was run simulating the plume of the SSMEs at an altitude of 15 km. This altitude was selected for study because the SSME plume is shockless. The nozzle exit conditions are from results obtained from the JANNAF Two-Dimensional Nozzle Performance Computer Program (TDK).<sup>26</sup>

Results are shown in Figure 4 for nitric oxide emission index and plume mean temperature as functions of  $x/r_0$ . Significant difference between the semi-equilibrium and the full-kinetic versions predictions can be seen. The afterburning reactions in the full-kinetic version are not near equilibrium; therefore, both nitric oxide production and mean plume temperature are affected by kinetics.

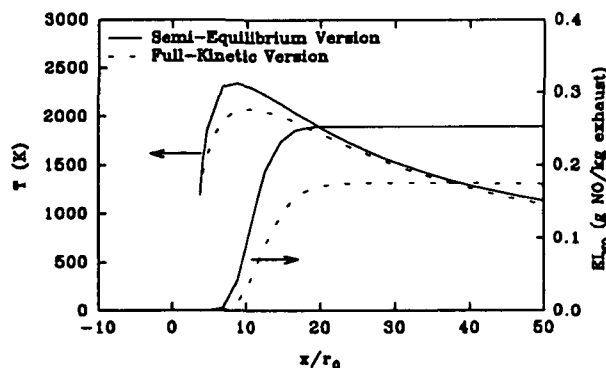


Figure 4. Nitric oxide production from plume afterburning in the SSME at an altitude of 15 km.

The plume emission indices and the estimated total production of nitric oxide for the two SSME test cases are shown in Table 4. A comparison of the semi-equilibrium version results with the Shuttle SRB estimates by Gomberg and Stewart (Table 4) shows that at an altitude of 15 km the two SRBs produce approximately 30 times more nitric oxide than do the three SSMEs.<sup>5</sup>

For altitudes near sea-level, the approximation of the nearfield nonisentropic shock/expansion system presents modeling difficulties. As an extreme test case,



we neglect the mass entrained in the viscous mixing process and also assume that the total energy of the flow at the nozzle exit-plane is conserved throughout the expansion. With the knowledge of the SSME nozzle exit-plane properties and an assumed final plume velocity, the initial temperature is calculated.

Table 4. SSME plume afterburning results. Unless otherwise noted  $E_t$  equals 0.16.

Altitude (km)	Final $EI_{NO}$ (g NO/ kg exhaust)	
	Full-Kinetic Version	Semi-Equilibrium Version
15		
$E_t$		
0.08	0.48	0.50
0.16	0.17	0.25
0.32	0.046	0.12
20	0.042	0.16
30	0.0033	0.014

The test case results are shown in Figure 5 for initial plume velocities from 1000 to 4500 m/s. The nitric oxide emission index increases with decreasing initial plume velocity, which is expected since the plume mean temperature and residence time increase with slower initial plume velocities. The full-kinetic version emission index increases about 6-fold for the plume initial velocity going from 4500 to 1000 m/s. For an initial velocity of 1000 m/s, the full-kinetic version estimates that the three SSMEs produce about 93 kg/s of nitric oxide and predicts the two Shuttle SRBs will produce nearly 190 kg/s of nitric oxide for operation at 0.7 km.

#### Stratospheric Plume Diffusion

The one-dimensional plume afterburning model analyzes the exhaust gases from the nozzle exit plane to a distance far downstream. The gas composition is modified through completion of combustion, chlorine activation, and nitric oxide production. Once the rocket plume slows, the gases advect, diffuse and react in the stratosphere. Species reactive with ozone attempt to destroy the ozone diffusing into the plume, producing a temporary local ozone deficit. The

analysis of the Stratospheric plume diffusion follows closely the work of Denison et al.<sup>8</sup>

For plume diffusion in the stratosphere, we employ the following assumptions:

1. Since it is well known that stratospheric mixing is turbulent; we neglect molecular diffusion.
2. Diffusion occurs predominantly in the horizontal direction.
3. The diffusion is axisymmetric with respect to a coordinate system moving at the mean wind speed.
4. There are no external sources or sinks of species, only chemical reactions.
5. Chemical reactions are driven by mean concentrations.

$$\frac{\partial n_i}{\partial t} = -\frac{1}{r} \frac{\partial}{\partial r} (\overline{u'_r n'_i}) + \dot{\omega}_i \quad (6)$$

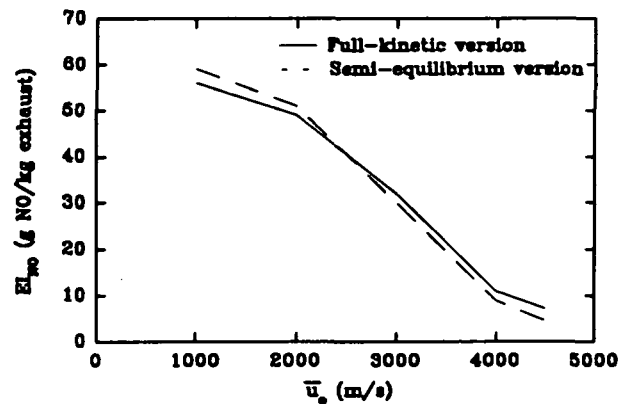


Figure 5. Variation of nitric oxide emission index with assumed initial velocity for SSME operating at 0.7 km.

Mathematical closure is obtained by modeling the correlation term. Accepted for stratospheric turbulent diffusion is an eddy or gradient diffusion model.<sup>27</sup> Eddy diffusion assumes species diffuse through gradients in concentration, analogous to molecular processes.

$$\overline{u'_r n'_i} = -K_{\pi} \frac{\partial n_i}{\partial r} \quad (7)$$

The eddy diffusion coefficient ( $K_{\pi}$ ) is an algebraic equation in terms of primary variables.

The determination of an accurate eddy diffusion model presents some difficulties. The plume size is much less than the characteristic size of turbulence in

the stratosphere. Following the work of Denison et al., we assume that the turbulent eddy coefficient is proportional to the radial location.<sup>8</sup>

$$K_{\pi} \propto r \quad (8)$$

For this work, two eddy coefficient models are studied:

$$1) K_{\pi} = KR_0 \quad 0 \leq r \leq \infty \quad (9)$$

$$2) K_{\pi} = KR_0 \quad 0 \leq r \leq R_0 \quad (10)$$

$$K_{\pi} = Kr \quad R_0 < r \leq \infty$$

The first model, equation 9, is a constant eddy coefficient model, and the second model, equation 10, is a dual eddy coefficient model. Values for the constant  $K$  are found to range from about 2 m/s for a curve-fit of stratospheric diffusion measurements to 7 m/s for calculations based upon Warneck's statistical theory.<sup>8</sup>

The mathematical model is a set of nonlinear coupled equations semi-infinite in space. To work in a finite spatial domain, the unbounded spatial variable ( $r$ ) is transformed to a bounded nondimensional spatial variable.

The chemical reactions and rate coefficients to be studied for local plume diffusion are tabulated in Table 5. Many of the reactions were also utilized by Denison et al. to model the chemistry of stratospheric diffusion.<sup>8</sup>

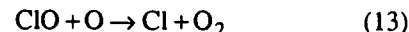
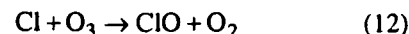
### Stratospheric Plume Diffusion Results and Discussion

The previous results for the Shuttle SRBs, Figure 3, show that a significant portion of the total chlorine is activated during plume afterburning. Negligible amounts of nitric oxide are produced in either the Shuttle SRBs or the SSMEs at or above 15 km; therefore, the dominant reactive species during local stratospheric plume diffusion are the active chlorine compounds,  $\text{Cl}$  and  $\text{Cl}_2$ .

The plume initial conditions and atmospheric conditions are listed in Table 6. The atmospheric conditions include the molar concentrations of all ambient species, the temperature and the pressure. Ozone molar concentration is from Warneck.<sup>27</sup>

The first test case looks at the chemical-kinetic mechanism dependence. The results from the plume afterburning model for the Shuttle SRB operating at 15 km are substituted into the diffusion model. The diffusion model is run twice: The first case utilizes the full chemical-kinetic mechanism listed in Table 5, while the second case employs only the photolysis of

diatomic chlorine and the two reactions describing the catalyst cycle of chlorine:



All test cases were run incorporating 250 grid points. The time step was set equal to 0.05 s.

The plume diffusion results are shown in Figure 6 for various centerline species as functions of time. The full chemical-kinetic mechanism estimates that, for  $K$  equal to 2 m/s, 720 s are required for the centerline ozone to reach 50% of the background (ozone recovery time). The three-reaction mechanism predicts it will take about 590 s; therefore, it appears that the local ozone is largely destroyed through reactions 11-13. Thus for a rough estimate of ozone recovery time, the full chemical-kinetic mechanism can be reduced to three primary reactions.

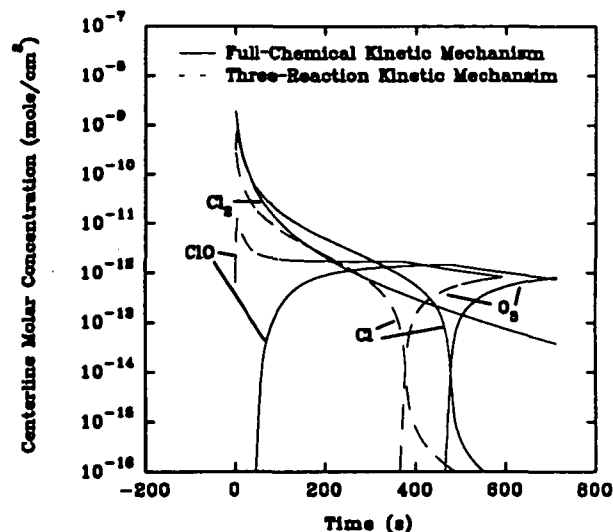


Figure 6. Plume diffusion for the Shuttle SRBs operating at 15 km.

The radial profiles of atomic chlorine, diatomic chlorine, and ozone, at several instants in time, are shown in Figure 7 for both the constant and dual eddy diffusion models utilizing the three-reaction mechanism. Initially, the chlorine species are a step profile, and the ozone is present outside the plume. Once diffusion begins, the chlorine diffuses outward and the ozone diffuses inward, with the catalyst reactions 11 and 12 occurring in the interface destroying ozone. The chlorine photolysis reaction appears as a source of the catalytic chlorine species

(Cl). It is apparent from Figure 7 that the mixed eddy diffusion model increases the rate of far-field ( $r$  greater than  $R_0$ ) diffusion. Eventually catalyst chlorine is reduced in concentration due to diffusion and chemical reactions, and the ozone diffuses back into the plume.

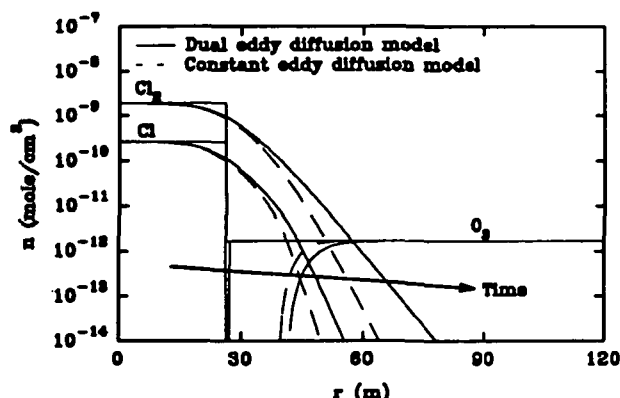


Figure 7. Plume diffusion predictions for the Shuttle SRBs operating at 15 km, concentration profiles shown at times equal to 0 and 0.55 s.

The major uncertainty in the diffusion model is the accuracy of the diffusion constant. Therefore, the model is exercised twice at each SRB operating altitude for the mixed eddy diffusion model utilizing both diffusion constants (2 and 7 m/s). Both the full chemical-kinetic mechanism and the three-reaction mechanism are tested, and the results are shown in Table 7.

To demonstrate the effect the diffusion model has on the results, one additional test case for the Shuttle SRB operating at 15 km is run with the constant eddy diffusion model. The results show that the ozone recovery time is nearly 4600 s, or about 46 times longer than the mixed eddy diffusion model predicts.

The ozone recovery time was shown by Denison et al. to increase with altitude for the hypothetical TRW SRM.<sup>8</sup> Contrary to Denison et al.'s findings, utilizing the one-dimensional plume afterburning model for initial conditions, the present results show that the minimum recovery time is at an altitude of 20 km. We found that the plume chlorine activation increases with altitude, but the diffusing plume initial radius increases with altitude. The result is that the initial chlorine concentration in the plume decreases with altitude; therefore, the ozone recovery time is affected by both plume size and chlorine activation. By increasing the diffusion constant ( $K$ ) from 2 to 7 m/s, the ozone recovery time increases by a factor of 5.

An additional test case was run using Denison et al.'s afterburning results from the hypothetical TRW SRM. The initial values are adjusted to reflect the size of the two Shuttle SRBs to obtain new plume initial conditions (Table 6). The results obtained using these initial conditions are listed in Table 7 and show a substantial increase in ozone recovery time over the results for the 30 km isentropically corrected initial conditions.

## Conclusions

Our one-dimensional plume afterburning models and the plume diffusion model provide insight into the affects afterburning can have on the exhaust gas.

We predict nitric oxide production decreases with altitude in the SRB plume, but active chlorine formation increases. At low altitudes, the one-dimensional model predicts significant nitric oxide production; above 15 km nitric oxide production is almost negligible. The full-kinetic version estimates qualitative emissions trends nearly identically to either Gombert and Stewart and Denison et al.<sup>5,8</sup> Additionally, the more recent chemical-kinetic mechanism predicts more chlorine activation than does Gombert and Stewart's mechanism. The full-kinetic version of the one-dimensional model shows that the corrected isentropic expanded properties have a negligible effect on chlorine activation until an altitude of about 30 km.

For SSME plume afterburning, the two chemical versions of the one-dimensional model do not predict identical plume nitric oxide results. The SSME plume produces negligible nitric oxide at 15 km or higher, but simple near-field plume approximations predict significant nitric oxide production near sea-level.

For the space shuttle SRB stratospheric plume diffusion, active chlorine compounds are the major species reacting with local ozone. Two reactions comprise the catalyst cycle destroying ozone; the third reaction predicts the photolysis of diatomic chlorine into the atomic catalyst form. Our predicted ozone recovery times range from a few minutes up to tens of minutes depending on the diffusion constant.

## Acknowledgements

This work was supported by the The Pennsylvania State University Propulsion Engineering Research Center under NASA grant NAGW-1356. D.M. Leone would also like to thank SwRI for their financial support and assistance in presenting this paper.

## References

1. Anon., *Space Shuttle Final Environmental Impact Statement*, NASA, April 1978.
2. Potter, A. E., "Proc. Space Shuttle Environmental Assessment Workshop on Stratospheric Effects," NASA TM X-58198, (1977).
3. Potter, A. E., "Environmental Effects of the Space Shuttle," *J. Environ. Sci.*, **21**, 15-21, (1978).
4. Anon., "Atmospheric Effects of Chemical Rocket Propulsion," Report of an AIAA Workshop, Sacramento, CA, 28-29 June, 1991, Draft July 1991.
5. Gomborg, R. I. and Stewart, R. B., "A Computer Simulation of the Afterburning Processes Occurring Within Solid Rocket Motor Plumes in the Troposphere," NASA-TN-8303, Dec. 1976.
6. Dash, S. M. et al., "Prediction of Rocket Plume Flowfields for Infrared Signature Studies," *J. Spacecraft* **17**, 3, (1980).
7. Dash, S. M. and Pergament, H. S., "The JANNAF Standard Plume Flowfield Model (SPF)," U.S. Army Missile Command, TR RD-CR-82-9, April 1981.
8. Denison, M. R. et al., "Solid Rocket Exhaust in the Stratosphere: Plume Diffusion and Chemical Reactions," AIAA paper No. 92-3399, (1992).
9. Seinfeld, J. H., *Atmospheric Chemistry and Physics of Air Pollution*, John Wiley & Sons, New York, (1986).
10. Anon., WMO Global Ozone Research and Monitoring Project Report No. 20, "Scientific Assessment of Stratospheric Ozone: 1989", (1989).
11. Aftergood, S., "Comment on 'The Space Shuttle's Impact on the Stratosphere' by Michael J. Prather et. al.," *J. Geophys. Res.* **96**(D9), 17,377, (1991).
12. McPeters, R., Prather, M. and Doiron, S., "Reply to Aftergood, S., Comment on 'The Space Shuttle's Impact on the Stratosphere' by Prather, M. et al.," *J. Geophys. Res.*, **95**(D9), 17,377, 1991., " *J. Geophys. Res.*, **95**(D9), 17,379-17,381, (1991).
13. Brasseur, G. and Solomon, S., *Aeronomy of the Middle Atmosphere*, Second Edition, D. Reidel, (1986).
14. Prather, M. et al., "The Space Shuttle's Impact on the Stratosphere," *J. Geophys. Res.*, **95**(D11), 18,583-18,590, (1990).
15. Turco, R. P., Toon, O. B., Whitten, R. C. and Cicerone, R. J., "Space Shuttle Ice Nuclei," *Nature*, **298**, 830-832, (1982).
16. Broadwell, J. E., "A Model of Turbulent Diffusion Flames and Nitric Oxide Generation: Part I and Part II," Final Report for Energy and Environmental Research Corporation, Contract No. PO18889, March 1982.
17. Lutz, A. E., "Simulation of Chemical Kinetics in Turbulent Natural Gas Combustion," Gas Research Institute Final Report, Contract No. 5089-260-1893, July 1992.
18. Ricou, F. I. and Spalding D. B., "Measurements of Entrainment by Axisymmetrical Turbulent Jets," *J. Fluid Mech.* **11**, 21, (1963).
19. Becker, H. A. and Yamazaki, S., "Entrainment, Momentum and Temperature in Vertical Free Turbulent Diffusion Flames," *Comb. and Flame* **33**, 123, (1978).
20. Miller, J. A. and Bowman, C. T., "Mechanism and Modeling of Nitrogen Chemistry in Combustion," *Progress Energy Combust Sci.* **15**, 4, (1989).
21. DeMore, W.B. et al., "Chemical Kinetics and Photochemical Data for Use in Stratospheric Modeling," NASA Panel Data Evaluation, JPL Publication 90-1, Jet Propulsion Laboratory, California Institute of Technology, (1990).
22. Reynolds, W. C., "STANJAN: The Element Potential Method for Chemical Equilibrium Analysis," Department of Mechanical Engineering, Stanford University, January 1986.
23. Kee, R. J., Rupley, F. M., and Miller, J. A., "CHEMKIN-II: A FORTRAN Chemical Kinetics Package for the Analysis of Gas-Phase Chemical Kinetics," Sandia Laboratories Report SAND89-8009 (1991).
24. Hindmarsh, A. C., "LSODE: Livermore Solver for Ordinary Differential Equations," Lawrence Livermore National Laboratory (1987).
25. Anon., "DGEAR", IMSL Library Reference Manual, IMSL, Inc., (1984).
26. Nickerson, G. R. et al., "Two-Dimensional Kinetics (TDK) Nozzle Performance Computer Program," Prepared for Marshall Space Flight Center, Contract No. NAS8-36863, Vol. 1-3, (1989).
27. Warneck, P., *Chemistry of the Natural Atmosphere*, Academic Press Inc, London, (1988).

Table 5. Chemical reactions describing active chlorine, odd nitrogen and odd hydrogen for the initial plume diffusion in the stratosphere.<sup>9,10,20</sup>

Chemical Reaction	$k_f = AT^N \exp(-E/RT)$				Ref.
	A ( $K^{-N}\cdot cm^3/molec\cdot s$ )	N	E/R ( K )		
<b>Catalyst Reaction</b>					
$Cl + O_3 \rightarrow ClO + O_2$	$2.9\cdot 10^{-11}$	0	-260		20
$ClO + O \rightarrow O_2 + Cl$	$3.0\cdot 10^{-11}$	0	-70		20
$NO + O_3 \rightarrow NO_2 + O_2$	$2.0\cdot 10^{-12}$	0	1400		20
$NO_2 + O \rightarrow NO + O_2$	$6.5\cdot 10^{-12}$	0	-120		20
$OH + O_3 \rightarrow HO_2 + O_2$	$1.6\cdot 10^{-12}$	0	940		20
$HO_2 + O \rightarrow OH + O_2$	$3\cdot 10^{-11}$	0	-200		20
<b>Photolysis Reaction</b>					
$Cl_2 + h\nu \rightarrow 2Cl$	Altitude Dependent (20-40 km) $\sim 3.0\cdot 10^{-3}$	0	0		9
<b>Inter-family Reaction</b>					
$2ClO + M \leftrightarrow Cl_2O_2 + M$	Low Pressure Limit $1.5\cdot 10^{-23}$	-3.6	0		20
$Cl_2O_2 + h\nu \rightarrow 2Cl + O_2$	Altitude Dependent (20 km) $\sim 1\cdot 10^{-3}$	0	0		10
$Cl_2O_2 + M \leftrightarrow 2ClO + M$	Low Pressure Limit $1\cdot 10^{-3}$	0	0		10
<b>Reaction between families</b>					
$ClO + NO_2 + M \rightarrow ClONO_2 + M$	Low Pressure Limit $4.7\cdot 10^{-23}$	-3.4	0		20
$ClONO_2 + h\nu \rightarrow Cl + NO_3$	Altitude Dependent (20 km) $\sim 5\cdot 10^{-5}$	0	0		9
$ClO + NO \rightarrow Cl + NO_2$	$6.4\cdot 10^{-12}$	0	-290		20
$ClO + HO_2 \rightarrow HOCl + O_2$	$4.8\cdot 10^{-13}$	0	-700		20
$HOCl + h\nu \rightarrow OH + Cl$	Altitude Dependent (20 km) $\sim 5\cdot 10^{-4}$	0	0		9
<b>Oxidation of CO</b>					
$OH + CO \rightarrow CO_2 + H$	$1.5\cdot 10^{-13}(1+0.6P_{Atm})$	0	0		20

Table 6. Initial and boundary conditions for plume diffusion of two Shuttle SRBs.

Property	Shuttle SRB Test Cases				
	15 km	20 km	30 km	30 km corrected	30 km Denison et al. <sup>8</sup>
T (K)	216	220	240	240	240
p (Atm)	0.11	0.057	0.014	0.014	0.014
R <sub>0</sub> (m)	26.4	37.4	83.5	85.2	85.2
Plume Initial Molar Concentration (mole/cm <sup>3</sup> )					
N <sub>2</sub>	2.66·10 <sup>-6</sup>	1.22·10 <sup>-6</sup>	3.2·10 <sup>-7</sup>	3.2·10 <sup>-7</sup>	3.2·10 <sup>-7</sup>
O <sub>2</sub>	6.85·10 <sup>-7</sup>	3.14·10 <sup>-7</sup>	8.2·10 <sup>-8</sup>	8.4·10 <sup>-7</sup>	8.4·10 <sup>-7</sup>
Cl <sub>2</sub>	1.90·10 <sup>-9</sup>	1.408·10 <sup>-9</sup>	5.13·10 <sup>-10</sup>	4.5·10 <sup>-10</sup>	5.46·10 <sup>-10</sup>
Cl	2.68·10 <sup>-10</sup>	4.48·10 <sup>-10</sup>	4.24·10 <sup>-10</sup>	2.04·10 <sup>-10</sup>	6.94·10 <sup>-10</sup>
ClO	3.90·10 <sup>-19</sup>	1.40·10 <sup>-18</sup>	3.09·10 <sup>-18</sup>	1.87·10 <sup>-15</sup>	
O	5.28·10 <sup>-19</sup>	2.68·10 <sup>-17</sup>	8.72·10 <sup>-16</sup>	5.90·10 <sup>-16</sup>	
O <sub>3</sub>	0.0	0.0	0.0	0.0	0.0
NO	1.08·10 <sup>-10</sup>	7.75·10 <sup>-12</sup>	1.78·10 <sup>-13</sup>	1.87·10 <sup>-13</sup>	
CO	1.17·10 <sup>-11</sup>	1.42·10 <sup>-11</sup>	1.21·10 <sup>-11</sup>	7.54·10 <sup>-11</sup>	
CO <sub>2</sub>	4.02·10 <sup>-8</sup>	1.98·10 <sup>-8</sup>	4.02·10 <sup>-9</sup>	3.89·10 <sup>-9</sup>	
Atmospheric Molar Concentration (mole/cm <sup>3</sup> )					
N <sub>2</sub>	2.66·10 <sup>-6</sup>	1.22·10 <sup>-6</sup>	3.2·10 <sup>-7</sup>	3.2·10 <sup>-7</sup>	3.2·10 <sup>-7</sup>
O <sub>2</sub>	6.85·10 <sup>-7</sup>	3.14·10 <sup>-7</sup>	8.2·10 <sup>-8</sup>	8.4·10 <sup>-7</sup>	8.4·10 <sup>-7</sup>
O <sub>3</sub>	1.66·10 <sup>-12</sup>	3.32·10 <sup>-12</sup>	5.0·10 <sup>-12</sup>	5.0·10 <sup>-12</sup>	5.0·10 <sup>-12</sup>

Table 7. Space Shuttle local plume diffusion results.

Test Case Condition	Ozone Recovery Time (s)				
	15 km	20 km	30 km	30 km corrected	30 km Denison et al. <sup>8</sup>
Dual Diffusion Model					
Full-Kinetic Mechanism					
K = 2 m/s	716	650	868	735	1040
K = 7 m/s	186	116	144	112	179
Three-Reaction Mechanism					
K = 2 m/s	591	518	663	584	
K = 7 m/s	103	89	134	107	
Const. Diffusion Model					
Three-Reaction Mechanism					
K = 7 m/s	4600				